CrossMark

Applied Mathematics and Nonlinear Sciences 1(1) (2016) 87–98

Applied Mathematics and Nonlinear Sciences

http://journals.up4sciences.org

Applications of the min-max symbols of multimodal maps

José M. Amigó†, Ángel Giménez.

Centro de Investigación Operativa, Universidad Miguel Hernández. Avda. de la Universidad s/n. 03202 Elche (Alicante).
Spain

Submission Info

Communicated by Juan L.G. Guirao
Received 24th June 2015
Accepted 17th December 2015
Available online 1st January 2016

Abstract

The min-max symbols generalize the kneading symbols in that they contain also information about the minimum or maximum character of the critical values and their iterates. Interestingly enough, this additional information can be obtained from the kneading symbols without further computation. In this paper we review some interesting applications of the min-max symbols. The applications chosen concern new expressions for the topological entropy of multimodal maps, as well as a numerical algorithm to compute it.

Keywords and phrases: Multimodal maps; min-max-symbols; topological entropy; numerical algorithm
2010 Mathematics Subject Classification: 37B40, 37E05, 37B10, 65Dxx

1 Introduction

The kneading sequences of a multimodal map f of a closed interval I are symbolic sequences that locate the iterates of its critical values up to the precision set by the partition defined by its critical points [15, 16]. See Sect. 2 for the exact meaning of these concepts in the present work and the general mathematical setting. Since the nth iterate of a critical point of f is a critical value of the nth iterate of f, f^n, one may attach to the symbols of each kneading sequence of f a label informing about their minimum/maximum (or "critical") character. The result is called a *min-max sequence*, one per critical point, consisting of min-max symbols. These symbols and sequences were introduced in [10, 11] for unimodal maps, and in [3] for multimodal maps. Thus, min-max sequences generalize kneading sequences in that they give additional geometric information about the extrema structure of f^n at the critical points for all $n \geq 1$. It turns out that the computational cost of a min-max

†Corresponding author.
Email address: jm.amigo@umh.es

ISSN 2444-8656 doi:10.21042/AMNS.2016.1.00008

symbol is virtually the same as of a kneading symbol. Indeed, the extra piece of information contained in each symbol of the min-max sequence generated by a critical point, as compared to the corresponding symbol of the kneading sequence generated by the same critical point, can be automatically retrieved from a look-up table once the min-max symbol of the previous iterate of f and the kneading symbol of the current iterate of f have been calculated.

The min-max symbols have been studied in recent years in the papers in [12] for twice-differentiable unimodal maps, in [3] for twice-differentiable multimodal maps, and in [4,5] for just continuous multimodal maps. Along with theoretical aspects, such as a number of relations between the min-max symbols of a unimodal or multimodal map and certain geometrical properties of the map and its iterates, the practical aspects were also on the fore in those references. In particular, several numerical algorithms for the topological entropy [1, 19] can be found as well in those references, the algorithm in [5] being a variant of the algorithm in [4] and this one a simplification of the algorithm in [3]. The interested reader is also referred to [6–9, 13, 14, 18] for several numerical techniques to compute the topological entropy with various degrees of generality.

In this paper we review two interesting applications of the min-max symbols of a multimodal map f, namely, new expressions for its topological entropy, $h(f)$, and a general algorithm to compute it. In so doing we resort to the well-known expression

$$h(f) = \lim_{n\to\infty} \frac{1}{n} \log \mathsf{lap}(f^n), \tag{1}$$

where $\mathsf{lap}(f^n)$ is shorthand for the *lap number* of f^n (i.e., the number of maximal monotonicity segments of f^n) [2, 17]. We will see in Sect. 3 that the min-max symbols allow to relate $\mathsf{lap}(f^n)$ with the number of 'transversal' intersections of f^n with the so-called critical lines. Let us also recall at this point other remarkable formulas such as

$$h(f) = \lim_{n\to\infty} \frac{1}{n} \log \#\{x \in I : f^n(x) = x\} \tag{2}$$

$$= \lim_{n\to\infty} \frac{1}{n} \log^{+} \mathsf{Var}(f^n), \tag{3}$$

where $\mathsf{Var}(f^n)$ stands for the variation of f^n [17].

The rest of this paper is organized as follows. In order to make the paper self-contained, we summarize in Sect. 2 all the basic concepts, especially the concept of min-max sequences, needed in the subsequent sections, and the concept of 'bad' symbols, which are the hallmark of this approach. In Sect. 3 we derive the two new expressions (11) and (19) for $h(f)$, which add to (1)-(3). A third expression, Eq. (22), is derived in Sect. 4 and, in turn, transformed into a numerical scheme to compute $h(f)$. The resulting algorithm is put to test with bimodal and trimodal maps in Sects. 4.1 and 4.2.

In sum, the following pages give a general panorama of the min-max symbols in action. For other applications of the min-max symbols the reader is referred to [3]. Further applications are the subject of current research.

2 Preliminaries

Let I be a compact interval $[a,b] \subset \mathbb{R}$ and $f : I \to I$ a piecewise monotone *continuous* map. Such a map is called l-modal if f has precisely l *turning points* (i.e., points in (a,b) where f has a local extremum). More precisely, we assume that f has local extrema at $c_1 < ... < c_l$ and that f is *strictly* monotone on each of the $l+1$ intervals

$$I_1 = [a, c_1), I_2 = (c_1, c_2), ..., I_l = (c_{l-1}, c_l), I_{l+1} = (c_l, b]. \tag{4}$$

The set of l-modal maps will be denoted hereafter as $\mathscr{M}_l(I)$, $\mathscr{M}_l([a,b])$, or just $\mathscr{M}_l$ if the interval $I = [a,b]$ is clear from the context or unimportant for the argument. As in the Introduction, sometimes one also speaks of multimodal maps in general, the name unimodal map being reserved for the case $l = 1$. Furthermore, if $f(c_1)$ is a maximum (resp. minimum), f is said to have a positive (resp. negative) shape.

The *itinerary* of $x \in I$ under f is a symbolic sequence

$$\mathbf{i}(x) = (i_0(x), i_1(x), ..., i_n(x), ...) \in \{I_1, c_1, I_2, ..., c_l, I_{l+1}\}^{\mathbb{N}_0}$$

($\mathbb{N}_0 \equiv \{0\} \cup \mathbb{N}$) defined as follows:

$$i_n(x) = \begin{cases} I_j \text{ if } f^n(x) \in I_j \ (1 \le j \le l+1), \\ c_k \text{ if } f^n(x) = c_k \ (1 \le k \le l). \end{cases}$$

The itineraries of the critical values,

$$\gamma^i = (\gamma_1^i, ..., \gamma_n^i, ...) = \mathbf{i}(f(c_i)),\ 1 \le i \le l,$$

are called the *kneading sequences* of f [15].

It is easily shown [3] that the iterates of the critical points, $f^n(c_i)$, are local extrema. This information is included in the *min-max sequences* of an l-modal map f,

$$\omega^i = (\omega_1^i, \omega_2^i, ..., \omega_n^i, ...),\ 1 \le i \le l,$$

where

$$\omega_n^i = \begin{cases} m^{\gamma_n^i} \text{ if } f^n(c_i) \text{ is a minimum}, \\ M^{\gamma_n^i} \text{ if } f^n(c_i) \text{ is a maximum}, \end{cases} \tag{5}$$

and γ_n^i are kneading symbols [3, 10–12]. Hence, the *min-max symbols* ω_n^i are a generalization of the kneading symbols γ_n^i in that they also specify whether $f^n(c_i)$ is a maximum or a minimum. In the exponential-like notation of (5), the 'base' belongs to the alphabet $\{m, M\}$, and the 'exponent' (also called signature in [3]) belongs to the alphabet $\{I_1, c_1, I_2, ..., c_l, I_{l+1}\}$. Therefore, the extra information of a min-max symbol ω_n^i as compared to a kneading symbol γ_n^i is contained in its base.

In [4, Theorem 1] it is proved that if $f \in \mathscr{M}_l$ has a positive shape, then the 'transition rules' given in Table 1 hold:

ω_n^i	$\to$	ω_{n+1}^i
$m^{I_{\text{odd}}}, M^{I_{\text{even}}}$	$\to$	$m^{\gamma_{n+1}^i}$
$m^{I_{\text{even}}}, M^{I_{\text{odd}}}$	$\to$	$M^{\gamma_{n+1}^i}$
$m^{c_{\text{even}}}, M^{c_{\text{even}}}$	$\to$	$m^{\gamma_{n+1}^i}$
$m^{c_{\text{odd}}}, M^{c_{\text{odd}}}$	$\to$	$M^{\gamma_{n+1}^i}$

Table 1 Transition rules for l-modal maps with a positive shape.

Here "even" and "odd" refer to the parity of the subindices of I_j $(1 \le j \le l+1)$ or c_k $(1 \le i \le l)$ in the exponent of ω_n^i. If, otherwise, f has a negative shape, then one has to swap m and M on the right column of Table 1 [4, Theorem 1]:

ω_n^i	$\to$	ω_{n+1}^i
$m^{I_{\text{odd}}}, M^{I_{\text{even}}}$	$\to$	$M^{\gamma_{n+1}^i}$
$m^{I_{\text{even}}}, M^{I_{\text{odd}}}$	$\to$	$m^{\gamma_{n+1}^i}$
$m^{c_{\text{even}}}, M^{c_{\text{even}}}$	$\to$	$M^{\gamma_{n+1}^i}$
$m^{c_{\text{odd}}}, M^{c_{\text{odd}}}$	$\to$	$m^{\gamma_{n+1}^i}$

Table 2 Transition rules for l-modal maps with a negative shape.

These transition rules prove our claim in the Introduction that, from the point of view of the computational cost, min-max sequences and kneading sequences are virtually equivalent.

Let the *ith critical line*, $1 \leq i \leq l$, be the line $y = c_i$ on the Cartesian plane $\{(x,y) : x,y \in \mathbb{R}\}$. Min-max symbols split into *bad* and *good symbols* with respect to the ith critical line. Geometrically, the latter correspond to local maxima strictly above the line $y = c_i$, and to local minima strictly below the line $y = c_i$. All other min-max symbols are bad by definition with respect to the ith critical line. We use the notation

$$\mathscr{B}^i = \{M^{I_1}, M^{c_1}, \dots, M^{I_i}, M^{c_i}, m^{c_i}, m^{I_{i+1}}, \dots, m^{c_l}, m^{I_{l+1}}\} \tag{6}$$

for the set of bad symbols of $f \in \mathscr{M}_l$ with respect to the ith critical line. There are $2(l+1)$ bad symbols and $2l$ good symbols with respect to a given critical line. Fig. 1 shows four bad min-max symbols with respect to the critical line $y = c_i$. Since the concept of bad symbol needs the minimum/maximum character of $f^n(c_i)$, it is a distinctive ingredient of properties derived via min-max symbols.

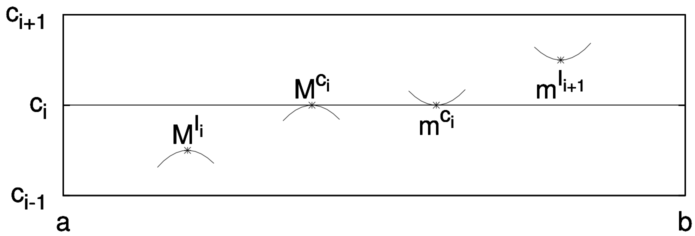

Fig. 1 Four bad symbols with respect to the critical line $y = c_i$. The rest are of the form M^{I_j}, M^{c_k} with $j,k < i$, and m^{I_j}, m^{c_k} with $j,k > i$.

For further reference, define the sets of pairs of indices

$$\mathscr{K}_n^i = \{(k,m), 1 \leq k \leq l, 1 \leq m \leq n : \omega_m^k \in \mathscr{B}^i\}, \tag{7}$$

($n \geq 1$, $1 \leq i \leq l$). That is, $\mathscr{K}_n^i$ collects the upper and lower indices (k,m), respectively, of the *bad* symbols with respect to the ith critical line in all the initial segments of length n of the min-max sequences of f:

$$\omega_1^1, \omega_2^1, \dots, \omega_n^1;\ \ \omega_1^2, \omega_2^2, \dots, \omega_n^2;\ \ \dots;\ \ \omega_1^l, \omega_2^l, \dots, \omega_n^l.$$

3 New expressions for the topological entropy

Let $f \in \mathscr{M}_l(I)$. Since f is continuous and piecewise strictly monotone, so is f^n for all $n \geq 2$ as well. We say that $x_0 \in I$ is an *interior simple zero of* $f^n(x) - c_i = 0$, $n \geq 0$, if $a < x_0 < b$, $f^n(x_0) = c_i$, and $f^n(x_0)$ is not a local extremum, thus $f^n(x)\ -c_i$ takes both signs in every neighborhood of x_0. In the case of (everywhere) differentiable maps, an interior simple zero x_0 of $f^n(x) - c_i = 0$ amounts geometrically to a *transversal* intersection on the two-dimensional interval $I \times I = \{(x,y) : x,y \in I\}$ of the curve $y = f^n(x)$ and the critical line $y = c_i$.

Let s_n^i, $1 \leq i \leq l$, stand for the *number of interior simple zeros of* $f^n(x) - c_i = 0$, $n \geq 0$. In order to simplify the notation, set

$$s_n = \sum_{i=1}^{l} s_n^i, \tag{8}$$

$n \geq 0$. In particular,

$$s_0 = \sum_{i=1}^{l} s_0^i = \sum_{i=1}^{l} 1 = l. \tag{9}$$

According to [3, Eqn. (31)], $\mathsf{lap}(f^n)$ satisfies

$$\mathsf{lap}(f^n) = 1 + \sum_{\nu=0}^{n-1} s_\nu. \tag{10}$$

Plug (10) into (1) to obtain

$$h(f) = \lim_{n\to\infty} \frac{1}{n} \log \left(1 + \sum_{\nu=0}^{n-1} s_\nu\right), \tag{11}$$

which expresses the topological entropy of a multimodal map f by means of the number of interior simple zeros of $f^n(x) - c_i = 0$, $1 \leq i \leq l$, or, in more geometrical terms, via the number of 'transversal' intersections of f^n with the critical lines, for $n \geq 1$.

For (11) to provide also a practical tool for computing $h(f)$, a procedure is needed to go from $s_0, s_1, ..., s_{n-1}$ to s_n. Here is where the min-max sequences of f enter the scene.

We say that an l-modal map f of the interval $I = [a,b]$ is *boundary-anchored* if $f\{a,b\} \subset \{a,b\}$, i.e., if

$$f(a) = a, \text{ and } f(b) = \begin{cases} a \text{ if } l \text{ is odd,} \\ b \text{ if } l \text{ is even,} \end{cases}$$

in case that f has a positive shape, or

$$f(a) = b, \text{ and } f(b) = \begin{cases} b \text{ if } l \text{ is odd,} \\ a \text{ if } l \text{ is even,} \end{cases}$$

in case that f has a negative shape.

Remark 1. It is well-known that when it comes to calculate the topological entropy of an l-modal map f, $h(f)$, then one may assume without restriction that f is boundary-anchored. Explicitly, given $f \in \mathscr{M}_l(I)$ there exist a closed interval $J \supset I$ and $F \in \mathscr{M}_l(J)$ such that $h(F) = h(f)$ and F is boundary-anchored; see, e.g., [4, Theorem 3] and the references therein.

Therefore, assume for the time being that $f \in \mathscr{M}_l$ is boundary-anchored. Then it is proved in [4, Theorem 2] that for any $n \geq 1$, $1 \leq i \leq l$,

$$s_n^i = 1 + \sum_{\nu=0}^{n-1} s_\nu - S_n^i, \tag{12}$$

where

$$S_n^i = 2 \sum_{(k,m)\in\mathscr{K}_n^i} s_{n-m}^k \tag{13}$$

with $S_n^i = 0$ if $\mathscr{K}_n^i = \emptyset$. Thus, see (8),

$$s_n = l\left(1 + \sum_{\nu=0}^{n-1} s_\nu\right) - S_n, \tag{14}$$

where

$$S_n = \sum_{i=1}^{l} S_n^i. \tag{15}$$

Note that the right hand of (12) only contains the numbers s_ν with $0 \leq \nu \leq n-1$, what allows to calculate s_n in a fully recursive way from the seeds $s_0^1 = ... = s_0^l = 1$. This fact and Remark 1 render Eq. (11) a formula for actually computing the topological entropy of *any* (i.e., not necessarily boundary-anchored) l-modal map f. Since the calculation of S_n^i involves the bad symbol set $\mathscr{K}_n^i$, the corresponding algorithm presupposes the knowledge of the min-max symbols ω_m^k with $1 \leq k \leq l$, and $1 \leq m \leq n$.

Remark 2. The generalization of (12) to general $f \in \mathscr{M}_l$, regardless of the boundary conditions, can be found in [3, Theorem 5.3].

The relation (14) not only promotes (11) to the basis of an algorithm for the computation of $h(f)$ via min-max symbols, but also leads to a further expression for $h(f)$. For this insert (10) in (14) to write the lap number $\mathsf{lap}(f^n)$ of a boundary-anchored l-modal map as

$$\mathsf{lap}(f^n) = \frac{1}{l}(s_n + S_n). \tag{16}$$

Next we derive from (16) a formula for $h(f)$ which involves the min-max symbols of f in an explicit manner. To this end we are going to express s_n in terms of $S_1, ..., S_n$.

Lemma 1. *[5]. Let $f \in \mathscr{M}_l$ be boundary-anchored. Then*

$$s_n = l(l+1)^n - l\sum_{\nu=1}^{n-1}(l+1)^{n-\nu-1}S_\nu - S_n \tag{17}$$

for $n \geq 1$, where the summation over ν is missing for $n = 1$.

From (16) and (17) it follows

$$\mathsf{lap}(f^n) = (l+1)^n\left(1 - \sum_{\nu=1}^{n-1}\frac{S_\nu}{(l+1)^{\nu+1}}\right) \tag{18}$$

for boundary-anchored l-modal maps. Apply now (1) to (18) and derive the following formula for the topological entropy of any l-modal map in virtue of Remark 1.

Theorem 2. *[5]. The topological entropy of $f \in \mathscr{M}_l$ is given by*

$$h(f) = \log(l+1) + \lim_{n\to\infty}\frac{1}{n}\log\left(1 - \sum_{\nu=1}^{n-1}\frac{S_\nu}{(l+1)^{\nu+1}}\right), \tag{19}$$

with S_ν as in (15) and (13).

According to (19) $h(f) \leq \log(l+1) =: h(f)_{\max}$, a well-known result for l-modal maps. Therefore, (19) expresses the difference $h(f)_{\max} - h(f)$ by means of the sequence $(S_n)_{n\geq 1}$. Note that the convergence is monotonic, i.e.,

$$\log(l+1) - \frac{1}{n}\left|\log\left(1 - \sum_{\nu=1}^{n-1}\frac{S_\nu}{(l+1)^{\nu+1}}\right)\right| \searrow h(f) \tag{20}$$

as $n \to \infty$. See [5, Sect. 5] for details of the convergence (20). The application of (19) to the logistic family,

$$q_v(x) = 4vx(1-x), \tag{21}$$

$0 \leq x \leq 1$, $0 < v \leq 1$, was extensively studied in [5, Sect. 6].

4 Computation of the topological entropy

In this section we are going to review a general algorithm to compute $h(f)$ [4]. This algorithm is based on the formula for $h(f)$ which follows readily from (1) and (16),

$$\begin{aligned} h(f) &= \lim_{n\to\infty}\frac{1}{n}\log\frac{1}{l}(s_n + S_n) \\ &= \lim_{n\to\infty}\frac{1}{n}\log\frac{1}{l}\sum_{i=1}^{l}\left(s_n^i + 2\sum_{(k,m)\in\mathscr{K}_n^i} s_{n-m}^k\right), \end{aligned} \tag{22}$$

again for any l-modal map f (Remark 1). All we need is a recursive scheme to compute the right hand side of (22) for ever larger n's.

The core of the algorithm consists of a loop over n. Each time the algorithm enters the loop, the values of s_{n-1} and S_{n-1} are updated to s_n and S_n, and the current estimation of $h(f)$ is compared to the previous one. Note that the computation of S_n^i, $1 \le i \le l$, requires $s_0^i = 1, s_1^i, \ldots, s_{n-1}^i$, see (13), while the computation of s_n^i, $1 \le i \le l$, requires $s_0^i, s_1^i, \ldots, s_{n-1}^i$, and S_n^i, see (12). Note also that $\mathscr{K}_n^i = \mathscr{K}_{n-1}^i \cup (\mathscr{K}_n^i \backslash \mathscr{K}_{n-1}^i)$, where

$$\mathscr{K}_n^i \backslash \mathscr{K}_{n-1}^i = \{(k,n), 1 \le k \le l : \omega_n^k \in \mathscr{B}^i\}. \tag{23}$$

We summarize next the algorithm resulting from (22) in the following scheme ("$A \longrightarrow B$" stands for "B is computed by means of A").

(A1) Parameters: $l \ge 1$ (number of critical points), $\varepsilon > 0$ (dynamic halt criterion), and $n_{\max} \ge 2$ (maximum number of loops).

(A2) Initialization: $s_0^i = 1$, and $\mathscr{K}_1^i = \{k, 1 \le k \le l : \omega_1^k \in \mathscr{B}^i\}$ $(1 \le i \le l)$.

(A3) First iteration: For $1 \le i \le l$,

$$\begin{array}{rll} s_0^i, \mathscr{K}_1^i & \longrightarrow S_1^i, S_1 & \text{(use (13), (15))} \\ s_0^i, S_1^i & \longrightarrow s_1^i, s_1 & \text{(use (12), (14))} \end{array}$$

(A4) Computation loop. For $1 \le i \le l$ and $n \ge 2$ keep calculating $\mathscr{K}_n^i$, S_n^i, and s_n^i according to the recursions

$$\begin{array}{rll} \mathscr{K}_{n-1}^i & \longrightarrow \mathscr{K}_n^i & \text{(use (23), and Table 1 or 2)} \\ s_0^i, s_1^i, \ldots, s_{n-1}^i, \mathscr{K}_n^i & \longrightarrow S_n^i, S_n & \text{(use (13), (15))} \\ s_0^i, s_1^i, \ldots, s_{n-1}^i, S_n^i & \longrightarrow s_n^i, s_n & \text{(use (12), (14))} \end{array} \tag{24}$$

until (i)

$$\left| \frac{1}{n} \log \frac{s_n + S_n}{l} - \frac{1}{n-1} \log \frac{s_{n-1} + S_{n-1}}{l} \right| \le \varepsilon, \tag{25}$$

or, else, (ii) $n = n_{\max} + 1$.

(A5) Output. In case (i) output

$$h(f) = \frac{1}{n} \log \frac{s_n + S_n}{l}. \tag{26}$$

In case (ii) output "Algorithm failed".

As a matter of course, the parameter ε does not bound the error $\left| h(f) - \frac{1}{n} \log \frac{s_n + S_n}{l} \right|$ but the difference between two consecutive estimations, see (25). The number of exact decimal positions of $h(f)$ can be found out by taking different ε's, as we will see in the numerical simulations below. Equivalently, one can control how successive decimal positions of $\frac{1}{n} \log \frac{s_n + S_n}{l}$ stabilize with growing n. Moreover, the smaller $h(f)$, the smaller ε has to be chosen to achieve a given numerical precision.

Remark 3. There are, of course, very efficient algorithms for the computation of $h(f)$ tailored to particular cases; for unimodal maps, see, e.g., [7]. Also in the unimodal case, the relation (16) leads easily to the recursive formula [12]

$$\mathsf{lap}(f^{n+1}) = 2\,\mathsf{lap}(f^n) - 2 \sum_{m \in \mathscr{K}_n^1} (\mathsf{lap}(f^{n+1-m}) - \mathsf{lap}(f^{n-m})), \tag{27}$$

$n \ge 1$, which allows to compute $h(f)$ in a simple and fast manner.

The algorithm (A1)-(A5) was benchmarked in [4] against (27) for unimodal maps and against the algorithm of [3] (also based on (22)) for l-modal maps with $2 \leq l \leq 5$. The result was that (27) is faster for unimodal maps, otherwise the algorithm (A1)-(A5) is faster. Let us mention in passing that (19) was used in [5] to derive a similar though slower computational scheme.

For the sake of completeness, we show next numerical results obtained with the above algorithm (A1)-(A5) applied to bimodal and trimodal maps. The algorithm was coded for arbitrary l with PYTHON and run on an Intel(R) Core(TM)2 Duo CPU. The base of the logarithm function is 2.

4.1 Bimodal maps

Consider the bimodal maps $f_{v_1,v_2} : [0,1] \to [0,1]$ defined as

$$f_{v_1,v_2}(x) = (2v_2 - v_1) - 2(v_2 - v_1)\sin\left(\frac{\pi}{6}\left(5 - 4\sqrt{6}x + 6x^2\right)\right),$$

where $0 \leq v_1 \neq v_2 \leq 1$. The critical points of f_{v_1,v_2} on the interval $[0,1]$ are

$$c_1 = \frac{1}{\sqrt{3}}(\sqrt{2} - 1) = 0.2391..., \quad c_2 = \sqrt{\frac{2}{3}} = 0.8165....$$

Moreover,

$$f_{v_1,v_2}(0) = v_2, \quad f_{v_1,v_2}(c_1) = v_1, \quad f_{v_1,v_2}(c_2) = v_2, \quad f_{v_1,v_2}(1) \begin{cases} > v_2 \text{ if } v_1 > v_2 \\ < v_2 \text{ if } v_1 < v_2 \end{cases}.$$

Therefore, if we choose $v_1 > v_2$, then f_{v_1,v_2} has a positive shape, while $v_1 < v_2$ entails a negative shape. Fig. 2 shows the graphs of the full range maps $f_{1,0}$ and $f_{0,1}$, together with $f_{0.75,0.25}$ and $f_{0.25,0.75}$.

Fig. 3 shows the plot of $h(f_{0,v_2})$ vs. v_2, $0 < v_2 \leq 1$, computed with $\varepsilon = 10^{-4}$ and $\Delta v_2 = 0.001$. Fig. 4 depicts the values of $h(f_{v_1,v_2})$ vs. v_1 and v_2, with $\varepsilon = 10^{-4}$ and $\Delta v_1 = \Delta v_2 = 0.01$. Finally, Table 3 illustrates the convergence of the algorithm (as measured by the number of computation loops) when calculating $h(f_{0.1,0.9})$. We see that $\varepsilon = 10^{-7}$ is necessary to fix the first two decimal positions.

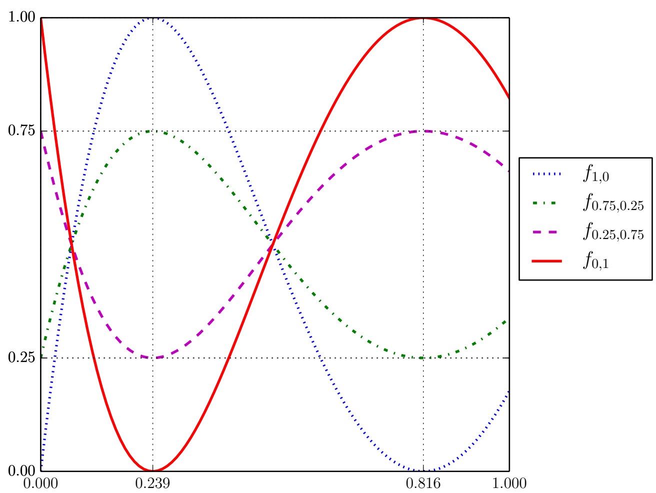

Fig. 2 Graph of the trimodal maps f_{v_1,v_2}

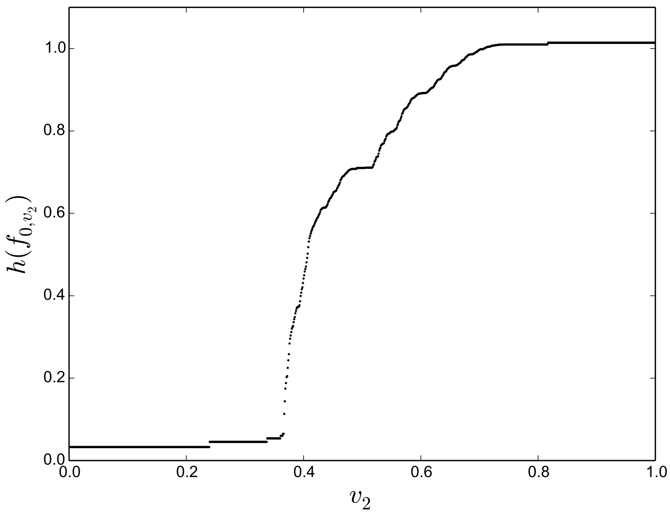

Fig. 3 Plot $h(f_{0,v_2})$ in bits vs v_2, $0 < v_2 \le 1$ ($\varepsilon = 10^{-4}, \Delta v_2 = 0.001$).

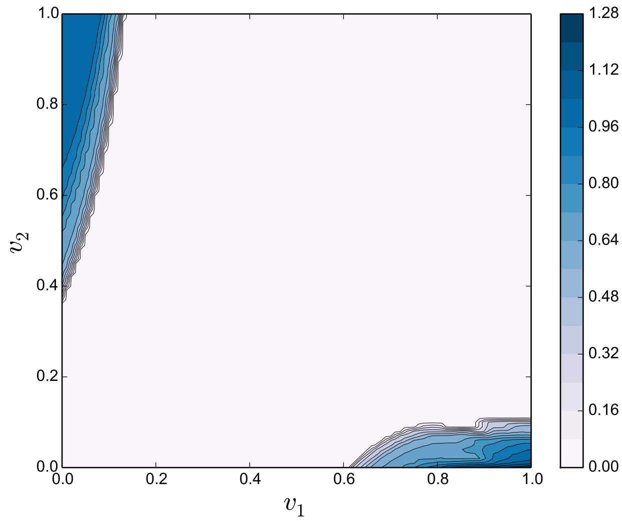

Fig. 4 Level sets of $h(f_{v_1,v_2})$ in bits vs v_1, v_2, $0 \le v_1, v_2 \le 1$ and $v_1 \ne v_2$ ($\varepsilon = 10^{-4}, \Delta v_1 = \Delta v_2 = 0.01$).

4.2 Trimodal maps

Consider the trimodal maps $g_{v_1,v_2} : [0,1] \to [0,1]$ defined as

$$g_{v_1,v_2}(x) = \frac{v_1 \cos\frac{\pi}{8} - v_2 + (v_2 - v_1)\sin\left(\frac{\pi}{8}\left(5 - 8x + 8x^2\right)\right)}{\cos\frac{\pi}{8} - 1},$$

where $0 \le v_1 \ne v_2 \le 1$. The critical points of g_{v_1,v_2} on the interval $[0,1]$ are

$$c_1 = \frac{1}{2}\left(1 - \frac{1}{\sqrt{2}}\right) = 0.1464..., \;\; c_2 = \frac{1}{2}, \;\; c_3 = \frac{1}{2}\left(1 + \frac{1}{\sqrt{2}}\right) = 0.8535...$$

Moreover,

$$g_{v_1,v_2}(0) = v_2, \quad g_{v_1,v_2}(c_1) = v_1, \quad g_{v_1,v_2}(c_2) = v_2, \quad g_{v_1,v_2}(c_3) = v_1, \quad g_{v_1,v_2}(1) = v_2.$$

precision	h	n
$\varepsilon = 10^{-4}$	0.655591287672	179
$\varepsilon = 10^{-5}$	0.643433302022	565
$\varepsilon = 10^{-6}$	0.639578859603	1786
$\varepsilon = 10^{-7}$	0.638359574751	5645

Table 3 Performances when computing $h(f_{0.1,0.9})$ in bits with the bimodal map.

As before, if we choose $v_1 > v_2$, then g_{v_1,v_2} has a positive shape, while $v_1 < v_2$ entails a negative shape. Fig. 5 shows the graphs of the full range maps $g_{1,0}$ and $g_{0,1}$, together with $g_{0.75,0.25}$ and $g_{0.25,0.75}$.

Fig. 6 shows the plot of $h(g_{0,v_2})$ vs. v_2, $0 < v_2 \leq 1$, computed with $\varepsilon = 10^{-4}$ and $\Delta v_2 = 0.001$. Fig. 7 depicts the values of $h(g_{v_1,v_2})$ vs. v_1 and v_2, with $\varepsilon = 10^{-4}$ and $\Delta v_1 = \Delta v_2 = 0.01$. Finally, Table 4 illustrates the convergence of the algorithm when calculating $h(g_{0.1,0.9})$. Here $\varepsilon = 10^{-6}$ fixes the first two decimal positions.

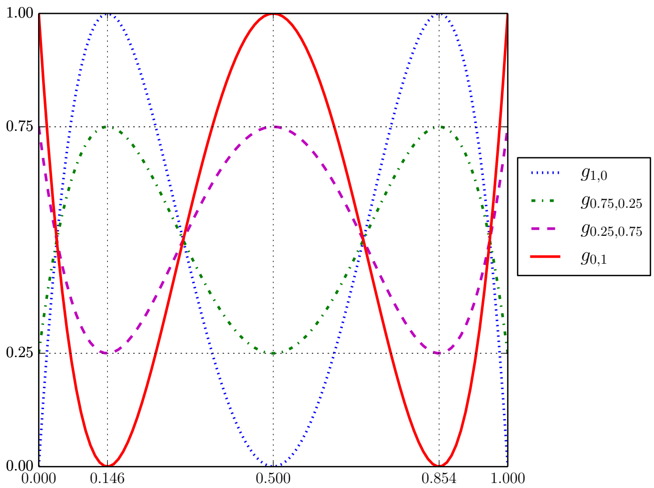

Fig. 5 Graph of the trimodal maps g_{v_1,v_2}

precision	h	n
$\varepsilon = 10^{-4}$	1.02013528493	203
$\varepsilon = 10^{-5}$	1.00638666069	640
$\varepsilon = 10^{-6}$	1.00202049572	2023
$\varepsilon = 10^{-7}$	1.00063926538	6394

Table 4 Performances when computing $h(g_{0.1,0.9})$ in bits with the trimodal map.

5 Conclusion

In this paper we have reviewed a few applications of the min-max symbols to both theoretical and computational aspects of the topological entropy of multimodal maps. Among the first, see Eqs. (19) and (22); among the latter, see the fast and numerically stable algorithm for $h(f)$ presented in Sect. 4, which is based on Eq. (22). The application of this algorithm to bimodal and trimodal maps was illustrated in Sect. 4 as well. The

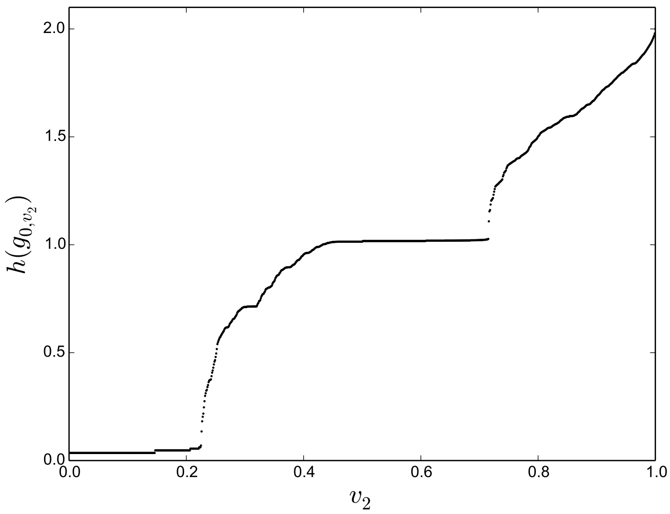

Fig. 6 Plot $h(g_{0,v_2})$ in bits vs v_2, $0 < v_2 \leq 1$ ($\varepsilon = 10^{-4}, \Delta v_2 = 0.001$).

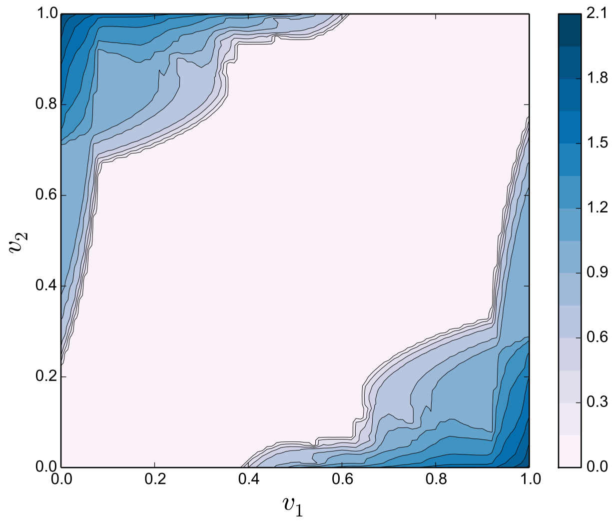

Fig. 7 Level sets of $h(g_{v_1,v_2})$ in bits vs v_1, v_2, $0 \leq v_1, v_2 \leq 1$ and $v_1 \neq v_2$ ($\varepsilon = 10^{-4}, \Delta v_1 = \Delta v_2 = 0.01$).

expressions (19), (22), and also (11) add to other well-known ones for $h(f)$ such as (1)-(3).

Acknowledgements

This work was financially supported by the Spanish Ministry of Economy and Competitiveness, grant MTM2012-31698.

References

[1] R. Adler, A. Konheim, and M. McAndrew, (1965), *Topological entropy*, Trans. Amer. Mat. Soc., 114, 309-319. doi 10.2307/1994177

[2] L. Alsedà, J. Llibre, and M. Misiurewicz, (2000), "*Combinatorial Dynamics and Entropy in Dimension One*", World Scientific, Singapore. doi 10.1142/9789812813367

[3] J.M. Amigó, R. Dilão, and A. Giménez, (2012), *Computing the topological entropy of multimodal maps via Min-Max sequences*, Entropy, 14, 742-768. doi 10.3390/e14040742

[4] J.M. Amigó and A. Giménez, (2014), *A Simplified algorithm for the topological entropy of multimodal maps*, Entropy, 16, 627-644. doi 10.3390/e16020627

[5] J.M. Amigó and A. Giménez, (2015), *Formulas for the topological entropy of multimodal maps based on min-max symbols*, Discrete and Continuous Dynamical Systems B, 20, 3415-3434. doi 10.3934/dcdsb.2015.20.3415

[6] S.L. Baldwin and E.E. Slaminka, (1997), *Calculating topological entropy*, J. Statist. Phys., 89, 1017-1033. doi 10.1007/BF02764219

[7] L. Block, J. Keesling, S. Li, and K. Peterson, (1989), *An improved algorithm for computing topological entropy*, J. Statist. Phys. **55**, 929-939. doi 10.1007/BF01041072

[8] L. Block and J. Keesling, (1991), *Computing the topological entropy of maps of the interval with three monotone pieces,* J. Statist. Phys., 66, 755-774. doi 10.1007/BF01055699

[9] P. Collet, J.P. Crutchfield, and J.P. Eckmann, (1983), *Computing the topological entropy of maps*, Comm. Math. Phys., 88, 257–262. doi 10.1007/BF01209479

[10] J. Dias de Deus, R. Dilão, and J. Taborda Duarte, (1982) *Topological entropy and approaches to chaos in dynamics of the interval*, Phys. Lett., 90A, 1-4. doi 10.1016/0375-9601(82)90033-0

[11] R. Dilão, (1985), *Maps of the interval, symbolic dynamics, topological entropy and periodic behavior* (in Portuguese), Ph.D. Thesis, Instituto Superior Técnico, Lisbon.

[12] R. Dilão and J.M. Amigó, (2012), *Computing the topological entropy of unimodal maps*, Int. J. Bifurc. and Chaos, 22, 1250152. doi 10.1142/S0218127412501520

[13] G. Froyland, R. Murray, and D. Terhesiu, (2007), *Efficient computation of topological entropy, pressure, conformal measures, and equilibrium states in one dimension*, Phys. Rev. E, 76, 036702. doi 10.1103/PhysRevE.76.036702

[14] P. Góra and A. Boyarsky, (1991), *Computing the topological entropy of general one-dimensional maps*, Trans. Amer. Math. Soc., 323, 39–49. doi 10.2307/2001614

[15] W. de Melo and S. van Strien, (1993) *One-Dimensional Dynamics* Springer, New York. doi 10.1007/978-3-642-78043-1

[16] J. Milnor and W. Thurston, (1988), *On iterated maps of the interval*, in "Dynamical Systems" (ed. J.C. Alexander), Lectures Notes in Mathematics, 1342, 465-563, Springer. doi 10.1007/BFb0082847

[17] M. Misiurewicz and W. Szlenk, (1980), *Entropy of piecewise monotone mappings*, Studia Math., 67, 45-63.

[18] T. Steinberger, (1999), *Computing the topological entropy for piecewise monotonic maps on the interval*, J. Statist. Phys., 95, 287–303. doi 10.1023/A:1004585613252

[19] P. Walters, (2000), *An Introduction to Ergodic Theory* Springer Verlag, New York. doi 10.1007/978-4-431-55060-0_22